The Plant Cell, Vol. 26: 4171–4187, October 2014, www.plantcell.org

Salicylic Acid Regulates *Arabidopsis* Microbial Pattern Receptor Kinase Levels and Signaling[W][OPEN]

Chika Tateda,[a,1] Zhongqin Zhang,[a,1] Jay Shrestha,[a] Joanna Jelenska,[a] Delphine Chinchilla,[b] and Jean T. Greenberg [a,2]

[a] Department of Molecular Genetics and Cell Biology, University of Chicago, Chicago, Illinois 60637
[b] Zurich-Basel Plant Science Center, Department of Environmental Sciences, University of Basel, 4056 Basel, Switzerland

In *Arabidopsis thaliana*, responses to pathogen-associated molecular patterns (PAMPs) are mediated by cell surface pattern recognition receptors (PRRs) and include the accumulation of reactive oxygen species, callose deposition in the cell wall, and the generation of the signal molecule salicylic acid (SA). SA acts in a positive feedback loop with ACCELERATED CELL DEATH6 (ACD6), a membrane protein that contributes to immunity. This work shows that PRRs associate with and are part of the ACD6/SA feedback loop. ACD6 positively regulates the abundance of several PRRs and affects the responsiveness of plants to two PAMPs. SA accumulation also causes increased levels of PRRs and potentiates the responsiveness of plants to PAMPs. Finally, SA induces PRR- and ACD6-dependent signaling to induce callose deposition independent of the presence of PAMPs. This PAMP-independent effect of SA causes a transient reduction of PRRs and ACD6-dependent reduced responsiveness to PAMPs. Thus, SA has a dynamic effect on the regulation and function of PRRs. Within a few hours, SA signaling promotes defenses and downregulates PRRs, whereas later (within 24 to 48 h) SA signaling upregulates PRRs, and plants are rendered more responsive to PAMPs. These results implicate multiple modes of signaling for PRRs in response to PAMPs and SA.

INTRODUCTION

Innate immunity in plants can be triggered through the action of receptor-like kinases at the cell surface, which can act as pattern recognition receptors (PRRs) upon binding microbial or self-derived molecules called pathogen-associated molecular patterns (PAMPs)/microbe-associated molecular patterns or damage/danger-associated molecular patterns, respectively (Jones and Dangl, 2006; Conrath, 2011). A well-studied PRR in *Arabidopsis thaliana* is FLAGELLIN SENSING2 (FLS2)/leucine-rich repeat receptor kinase, which recognizes the flg22 peptide derived from bacterial flagellin (Gómez-Gómez and Boller, 2000; Chinchilla et al., 2006). flg22 binding rapidly induces FLS2 to interact with its signaling partner, BRI1-ASSOCIATED RECEPTOR KINASE1 (BAK1) (Chinchilla et al., 2007; Heese et al., 2007). FLS2 interactions with BAK1 also result in the phosphorylation of both partners (Schulze et al., 2010), reactive oxygen species (ROS) accumulation, and the activation of several kinases, including mitogen-activated protein kinases (MAPKs; also called MPKs) and Ca^{2+}-dependent protein kinases (Boller and Felix, 2009; Boudsocq et al., 2010; Schwessinger et al., 2011). Subsequently, flg22 induces transcriptional reprogramming and callose deposition to strengthen cell walls (Boller and Felix, 2009). After flg22 stimulation, FLS2 is endocytosed from the plasma membrane and downregulated (Robatzek et al., 2006; Beck et al., 2012; Smith et al., 2014).

In *Arabidopsis*, another pair of PAMP and PRR is elf18 (for peptide elicitor from bacterial EF-Tu)/EFR (for EF-Tu receptor) (Zipfel et al., 2006). CHITIN ELICITOR RECEPTOR KINASE (CERK1)/LYSM DOMAIN RECEPTOR-LIKE KINASE1 is a PRR that can be activated by two PAMPs, chitin from fungi and peptidoglycan from bacteria (Miya et al., 2007; Petutschnig et al., 2010; Willmann et al., 2011). These pathways, when activated, share with flg22-stimulated responses some common signaling events, although the magnitude and kinetics of responses to different PAMPs can vary (Boller and Felix, 2009; Ranf et al., 2011).

Treatment with flg22 leads to the accumulation of the phytohormone ethylene (Boller and Felix, 2009) and the defense signal molecule salicylic acid (SA) (Mishina and Zeier, 2007; Tsuda et al., 2008). The basal transcript level of FLS2 requires the perception of endogenous ethylene, which also maintains FLS2 levels in a feedback loop of flg22 treatment (Boutrot et al., 2010; Mersmann et al., 2010). SA regulates defenses that are effective against many pathogens (Delaney et al., 1994; Lawton et al., 1996; Wildermuth et al., 2001; Murphy and Carr, 2002; Love et al., 2007; Chen et al., 2009; Wang et al., 2013). SA or SA agonists such as benzo(1,2,3)thiadiazole-7-carbothioic acid (BTH) (Friedrich et al., 1996; Görlach et al., 1996; Lawton et al., 1996) induce signaling that can directly lead to defense responses such as transcriptional reprogramming (Moore et al., 2011) and callose deposition in the cell wall (Kohler et al., 2002; Wang et al., 2013). Additionally, SA or BTH treatment can potentiate responses to various stimuli, including pathogens and PAMPs. For example, SA enhances flg22-triggered ROS accumulation (Sato et al., 2010; Xu et al., 2014). Potentiation may be aided by SA signaling-induced

[1] These authors contributed equally to this work.
[2] Address correspondence to jgreenbe@uchicago.edu.
The author responsible for distribution of materials integral to the findings presented in this article in accordance with the policy described in the Instructions for Authors (www.plantcell.org) is: Jean T. Greenberg (jgreenbe@uchicago.edu).
[W] Online version contains Web-only data.
[OPEN] Articles can be viewed online without a subscription.
www.plantcell.org/cgi/doi/10.1105/tpc.114.131938

increases specifically in the plasma membrane pools of the PRRs FLS2 and BAK1 (Zhang et al., 2014). SA signaling is also required for both local and systemic disease resistance that is induced after a local application of flg22 (Mishina and Zeier, 2007; Tsuda et al., 2008).

Among SA regulators, the *Arabidopsis* endoplasmic reticulum and plasma membrane protein ACCELERATED CELL DEATH6 (ACD6) acts in a positive feedback loop with SA to stimulate defenses and confer disease resistance (Lu et al., 2003, 2005). The dominant gain-of-function allele of ACD6 called *acd6-1* (Rate et al., 1999), which encodes an L591F amino acid substitution in a predicted transmembrane helix of ACD6, causes increased accumulation of the ACD6-1 protein and SA in *acd6-1* (Vanacker et al., 2001; Lu et al., 2003). *acd6-1* also shows autoimmunity phenotypes, which include reduced stature, small cell death patches, ectopic callose accumulation, and enhanced resistance to *Pseudomonas syringae* and *Hyaloperonospora parasitica* (Rate et al., 1999; Lu et al., 2005). Natural gain-of-function alleles of *ACD6* from different *Arabidopsis* accessions partially phenocopy *acd6-1*, and they confer enhanced resistance to several pathogens (Todesco et al., 2010). By contrast, plants that lack ACD6 show enhanced disease susceptibility and a delay in SA accumulation during *P. syringae* infection (Lu et al., 2003). ACD6 associates with FLS2 (Zhang et al., 2014), which suggests that there may be a direct relationship between ACD6/SA, FLS2, and other well-studied PAMP receptors.

In this study, we exploited both loss- and gain-of-function mutants of ACD6, as well as the SA agonist BTH, to study the regulation and functions of FLS2, BAK1, and CERK1. We report that ACD6 and SA regulate signaling events induced by PAMPs by influencing the levels of receptors and a coreceptor. Additionally, we show that, like ACD6, FLS2, BAK1, and CERK1 all contribute to signaling in the response to SA and/or an SA agonist in the absence of PAMPs.

RESULTS

acd6-1 and BTH-Treated Wild-Type Plants Show Potentiated ROS Production and Callose Deposition in Response to flg22

SA enhances flg22-triggered ROS accumulation (Sato et al., 2010; Xu et al., 2014). Since *acd6-1* accumulates high levels of SA (Vanacker et al., 2001), it seemed possible that SA signaling might affect the responses of *acd6-1* plants to flg22. Figures 1A to 1D and Supplemental Figures 1A and 1B (and similar diagrams in other figures) show treatment designs for testing this possibility using measurements of ROS accumulation and callose deposition. The timing of the treatments was designed to allow plant material to be collected under similar light conditions and to minimize changes in physiology. Previous work showed that for soil-grown plants, a water pretreatment of excised tissue was needed to detect an flg22-induced ROS response (Felix et al., 1999; Flury et al., 2013). However, the long water pretreatments that are typically used can mask mutant phenotypes, making long pretreatments unsuitable for assessing the basal state of some plants. For example, the *etr1-1* ethylene receptor mutant that normally has reduced responsiveness to flg22 regained full responsiveness to flg22 after overnight (long) water pretreatment (Mersmann et al., 2010). We sought to minimize the water pretreatment time, since high humidity suppresses SA-dependent autoimmune phenotypes in several mutants with constitutive SA accumulation (similar to *acd6-1*) (Jambunathan et al., 2001; Yoshioka et al., 2001; Zhou et al., 2004; Mosher et al., 2010). SA-induced gene expression is also inhibited by high humidity (Zhou et al., 2004). After only 4 h of water treatment, we could observe flg22-induced ROS in the wild type (Figures 1E and 1F). Importantly, unlike the results with long water pretreatment (Mersmann et al., 2010), the 4-h water treatment permitted the reduced responsiveness of *etr1-1* to flg22 to be readily detected (Supplemental Figure 1F). Therefore, we used 4-h pretreatments.

After flg22 treatment, ROS production was initiated faster and showed a higher total level in *acd6-1* relative to the wild type (Figures 1E and 1F). The starting time and peak accumulation time of ROS occurred 1 and 5 min earlier, respectively, in *acd6-1* than in wild-type plants (Figure 1E). In *fls2* and *acd6-1 fls2* mutants, which were used as negative controls, ROS did not accumulate in response to flg22 (Figure 1F). Relative to the wild type, flg22 caused more callose deposition in *acd6-1* (Figure 1G). Additionally, *acd6-1* accumulated callose deposits before treatment (Lu et al., 2005) at a level similar to that seen in flg22-treated wild-type plants. To test whether the potentiation of flg22 responses in *acd6-1* was due to high endogenous SA accumulation, we studied *acd6-1 sid2-1* plants, in which SA levels are greatly reduced due to *sid2-1* (Nawrath and Métraux, 1999; Lu et al., 2009). Both flg22-induced callose deposition and total ROS accumulation were reduced in *acd6-1 sid2-1* relative to *acd6-1* (Figures 1G and 1H). The enhanced response of *acd6-1* relative to the wild type was suppressed by prolonged incubation in water prior to flg22 treatment (Supplemental Figure 1G), consistent with *acd6-1*'s phenotype (and possibly SA accumulation) being suppressed by high humidity. This suggests that enhancement of the flg22 response in *acd6-1* required elevated SA levels.

SA agonists potentiate defense responses in a manner similar to SA (Conrath et al., 1995; Friedrich et al., 1996; Görlach et al., 1996; Lawton et al., 1996). Therefore, we also tested whether the SA agonist BTH affected responses to flg22. Indeed, callose deposition in response to flg22 was enhanced in wild-type plants pretreated for 24 h with BTH (Figure 1I). Additionally, flg22-induced accumulation of ROS in the wild type was enhanced by 24 h of BTH pretreatment (Figure 1J). However, unlike in the *acd6-1* plants, in these conditions, SA or BTH treatment did not affect the timing of the initiation of flg22-induced ROS production (Sato et al., 2010; Xu et al., 2014) (Figure 1K). *acd6-1 sid2-1* and *acd6-1* plants responded to flg22 with the same timing of ROS production (Figure 1H, right panel). Thus, the increased magnitude of flg22 responses in *acd6-1* and BTH-treated wild-type plants is caused by SA or an SA agonist, but the change in the timing of ROS accumulation in *acd6-1* is independent of SA.

acd6-1 and BTH-Treated Wild-Type Plants Show Enhanced Responsiveness to flg22 Due to High FLS2 and BAK1 Levels

flg22 binds to, and the cellular responses depend on, the receptor complex formed by FLS2 and BAK1 (Gómez-Gómez and Boller,

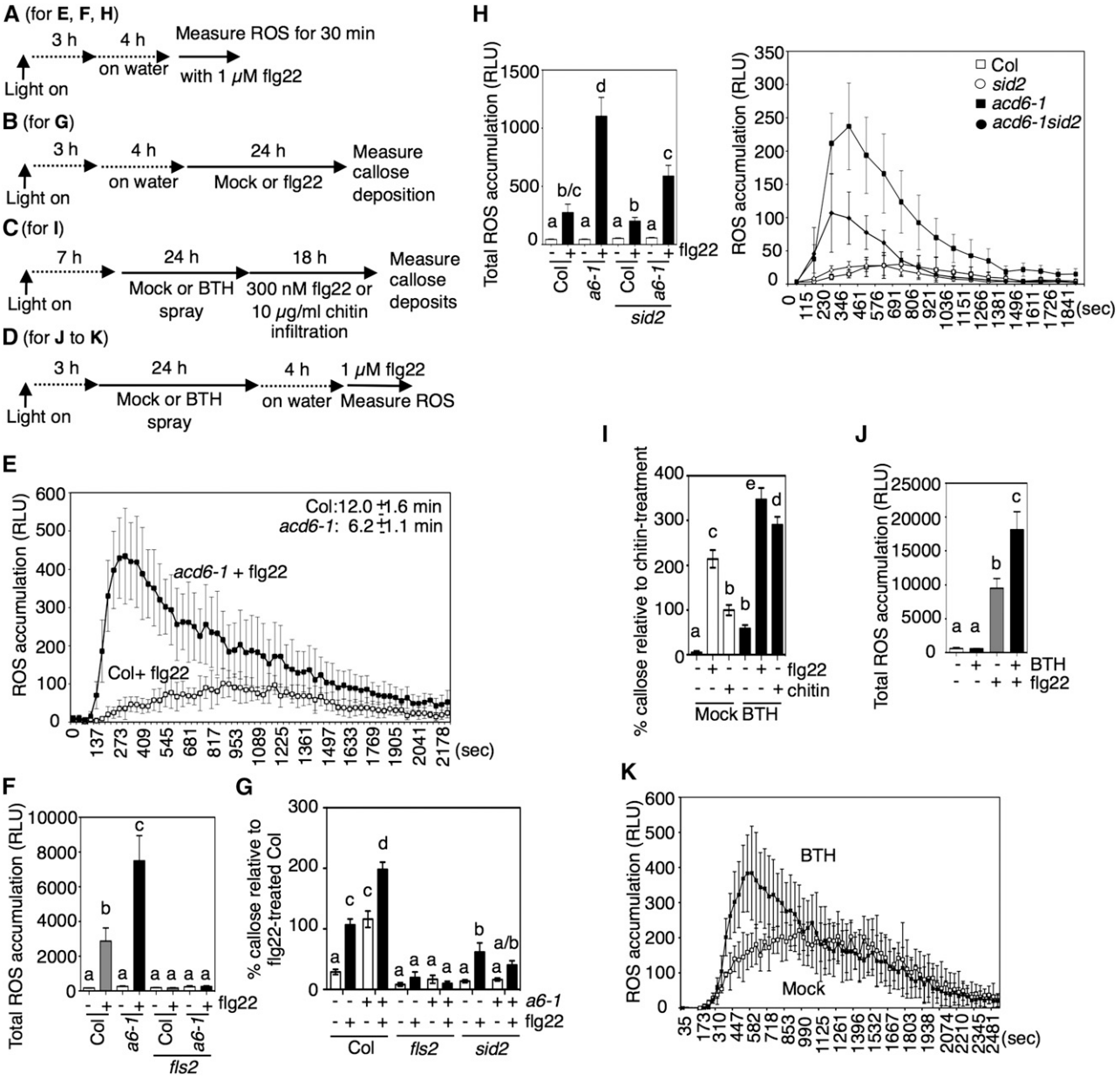

Figure 1. The flg22 Response Is Enhanced in *acd6-1* and the Wild Type after 24 h of BTH Treatment.

(A) to **(D)** Chemical treatment schemes for the indicated panels: **(A)** for **(E)**, **(F)**, and **(H)**; **(B)** for **(G)**; **(C)** for **(I)**; **(D)** for **(J)** and **(K)**. In **(A)**, **(B)**, and **(D)**, "on water" indicates that tissue was excised and floated on water to facilitate flg22 uptake.

(E) and **(F)** ROS accumulation after 1 μM flg22 treatment of the indicated plants ($n > 6$). The times of the ROS accumulation peaks in the wild type (Col) and *acd6-1* (*a6-1*) are is shown in the top right corner **(E)**; – or + indicates the absence or presence of flg22 **(F)**.

(G) Callose deposition in leaves of the indicated plant lines ($n > 24$) as a percentage of the flg22-treated wild type (Col). – or + indicates without or with *acd6-1* and absence or presence of flg22.

(H) ROS accumulation after 1 μM flg22 treatment in the indicated plants. The graph shows total ROS accumulation after 1 μM flg22 treatment.

(I) Callose deposition after mock, 1 μL flg22, or 10 μg/mL chitin treatment in wild-type plants pretreated for 24 h with 100 μM BTH or water as a percentage of chitin-treated plants ($n > 30$).

(J) Total ROS accumulation after 1 μM flg22 treatment in wild-type plants pretreated for 24 h with 100 μM BTH or water ($n = 12$).

(K) ROS accumulation after 1 μM flg22 treatment in wild-type plants pretreated for 24 h with 100 μM BTH or water ($n = 6$).

RLU, relative light units. Error bars in **(E)**, **(F)**, **(H)**, **(J)**, and **(K)** are SD of data from representative experiments. Error bars in **(G)** and **(I)** are SE of data from three independent experiments analyzed together. Except for the experiments in **(H)**, which were repeated twice, all experiments were repeated three times with similar results. Letters above bars represent significance groups as determined by the Newman-Keuls multiple comparison test, $P < 0.05$ or better (**[F]** to **[J]**).

2000; Chinchilla et al., 2006; Sun et al., 2013). Therefore, we evaluated the levels of FLS2 and BAK1 in plants that showed increased responsiveness to flg22. Figures 2A and 2B and Supplemental Figures 1C to 1E show the timing and treatments used for evaluating PRR levels. Forty-eight hours after spraying BTH on wild-type leaves, FLS2 and BAK1 levels were increased in both the microsomal membrane fraction and the total leaf extracts when compared with mock-treated samples (Figure 2C; Supplemental Figure 1H). BTH also induced elevated membrane levels of FLS2 and BAK1 at 24 h (Supplemental Figure 1I). Thus, the increased responsiveness of BTH-treated plants to flg22 parallels the increased receptor levels.

The levels of FLS2 and BAK1 were increased in total extracts and microsomal membrane fractions from *acd6-1* plants relative to those found in the wild-type accession Columbia (Col) (Figure 2D). To test whether the elevated receptor levels in *acd6-1* were due to the high accumulation of SA, we made use of the *sid2-1* mutation. This mutation does not significantly affect basal SA levels (relative to Col), but it greatly decreases SA levels when crossed into the *acd6-1* background (Lu et al., 2009) or during infection (Nawrath and Métraux, 1999). FLS2 and BAK1 levels were reduced in the microsomal membrane fraction of *acd6-1 sid2-1* relative to *acd6-1* (Figure 2E). Quantitative immunoblots showed that BAK1, but not FLS2, was still somewhat increased in *acd6-1 sid2-1* relative to *sid2-1* (Figure 2E, graphs). Possibly some other factor, or the ACD6-1 protein itself, regulates the residual pool of BAK1 in *acd6-1 sid2-1*. The levels of FLS2 and BAK1 in *sid2-1* were found to be similar to those in Col when quantified using three independent experiments (Figure 2E, graphs).

The basal level of FLS2 in the wild type requires an intact ethylene-signaling pathway (Boutrot et al., 2010; Mersmann et al., 2010). As reported previously (Mersmann et al., 2010), plants in which ethylene signaling was blocked due to the *etr1-1* receptor mutation (Chang et al., 1993) had very low FLS2 levels (Figure 2F). It seemed possible that ethylene also contributed to FLS2 regulation in *acd6-1*. The level of *ERF1* transcript, a marker for ethylene signaling (Berrocal-Lobo et al., 2002), was higher in *acd6-1* than in Col, indicating activation of the ethylene pathway in *acd6-1* (Figure 2G). However, in *acd6-1 etr1-1* plants, membrane levels of FLS2 and BAK1 were similar to those found in *acd6-1* plants (Figure 2F). Thus, elevated levels of BAK1 and FLS2 in *acd6-1* were not a consequence of increased ethylene signaling.

As discussed above, the levels of FLS2 and BAK1 were elevated in *acd6-1* relative to the wild type in extracts prepared from directly harvested tissue (Figure 2D). We sought to also assess the levels of these receptors under the same conditions used for the experiments in Figure 1, where we evaluated the flg22 responses of *acd6-1* and which involved floating tissue on water for 4 h prior to flg22 application. This water pretreatment step was proposed to remove wounding stress resulting from excising the leaves (Flury et al., 2013). Water pretreatment for 4 h after excising leaf tissue caused increased receptor levels in total extracts of the wild type but had more modest effects on the levels in the membrane fractions (Supplemental Figure 1J). FLS2 also accumulated after 4 h of water spray treatment without wounding (Supplemental Figure 1K). Accumulation of FLS2 in response to water treatment is consistent with a previous report that immunity-related (also flg22/FLS2) WRKY22 and FRK1 transcripts are also induced by submergence (Hsu et al., 2013). After pretreatment, the levels of FLS2 and BAK1 in *acd6-1* total extracts were also affected, but to a lesser extent (Supplemental Figure 1J). More importantly, we consistently found that the levels of FLS2 and BAK1 in the membrane fractions of *acd6-1* extracts were higher than those found in the wild type after 4 h of water treatment of the tissues (Supplemental Figure 1J). Thus, the increased responsiveness of *acd6-1* plant tissue to flg22 (Figure 1) occurred when high levels of FLS2 and BAK1 were present in the membrane fractions (Supplemental Figure 1J).

FLS2 and BAK1 Contribute to Autoimmune Signaling in *acd6-1*

Since *acd6-1* confers activation of ectopic callose deposition (Lu et al., 2003; Figure 1G) and showed increased receptor levels (Figure 2D), we assayed several PRR-related signaling events in *acd6-1* and their possible dependencies on FLS2 and BAK1. Figures 3A and 3B show the timing and treatments used for testing the PRR-related signaling events in *acd6-1*. We focused on responses typically induced by PAMPs (MAPK activation, expression of At1g51890, and callose accumulation) as well as more general SA-related defenses (*PR1* transcript accumulation, SA levels, and cell death).

In *acd6-1*, levels of MPK3, MPK6, and phosphorylated MPK3 and MPK6 were elevated (Figure 3C; Supplemental Figure 2; Zhang et al., 2014). High levels of MPK3 and MPK6 were anticipated, as BTH treatment of wild-type plants induces these proteins, but not their phosphorylated forms, to accumulate (Beckers et al., 2009). MPK6 levels were modestly reduced, but MPK3 and phosphorylated MPK3 and MPK6 levels were not significantly reduced in *acd6-1 fls2* or *acd6-1 bak1-4* relative to *acd6-1* (Figure 3C, graphs). Possibly, the high levels of activated MPK3 and MPK6 are due to other defense components activated in *acd6-1* (Lu et al., 2009).

The *fls2* and *bak1-4* mutations had a considerable effect on some defenses in *acd6-1*, because the double mutants showed a reduction in *At1g51890* transcript levels and callose deposition when compared with the single *acd6-1* mutant (Figures 3D and 3E). The transcript level of *PR1* was also significantly reduced in *acd6-1 fls2* and *acd6-1 bak1-4* relative to *acd6-1* (Figure 3F). Interestingly, SA accumulation was also modestly reduced by 25 to 30% in *acd6-1 fls2* versus *acd6-1* plants (Figure 3G). *acd6-1*-conferred cell death was also reduced in *acd6-1 fls2* or *acd6-1 bak1-4* mutants relative to *acd6-1* (Figure 3H).

Activation of FLS2-mediated signaling by the flg22 ligand involves complex formation with BAK1 (Chinchilla et al., 2007; Heese et al., 2007). To test whether FLS2-BAK1 complexes might contribute to autoimmune signaling or affect ligand-induced signaling in *acd6-1*, we performed coimmunoprecipitation experiments. There were weak immunoblot signals for FLS2 in the wild type after flg22 treatment and BAK1 immunoprecipitation (10 min; Figure 3I) that we interpret as low levels of FLS2-BAK1 complex formation under our experimental conditions from adult *Arabidopsis* leaves. By contrast, *acd6-1* showed FLS2 signals after BAK1 immunoprecipitation in samples collected from both mock and flg22 samples (Figure 3I). However, when tissues were

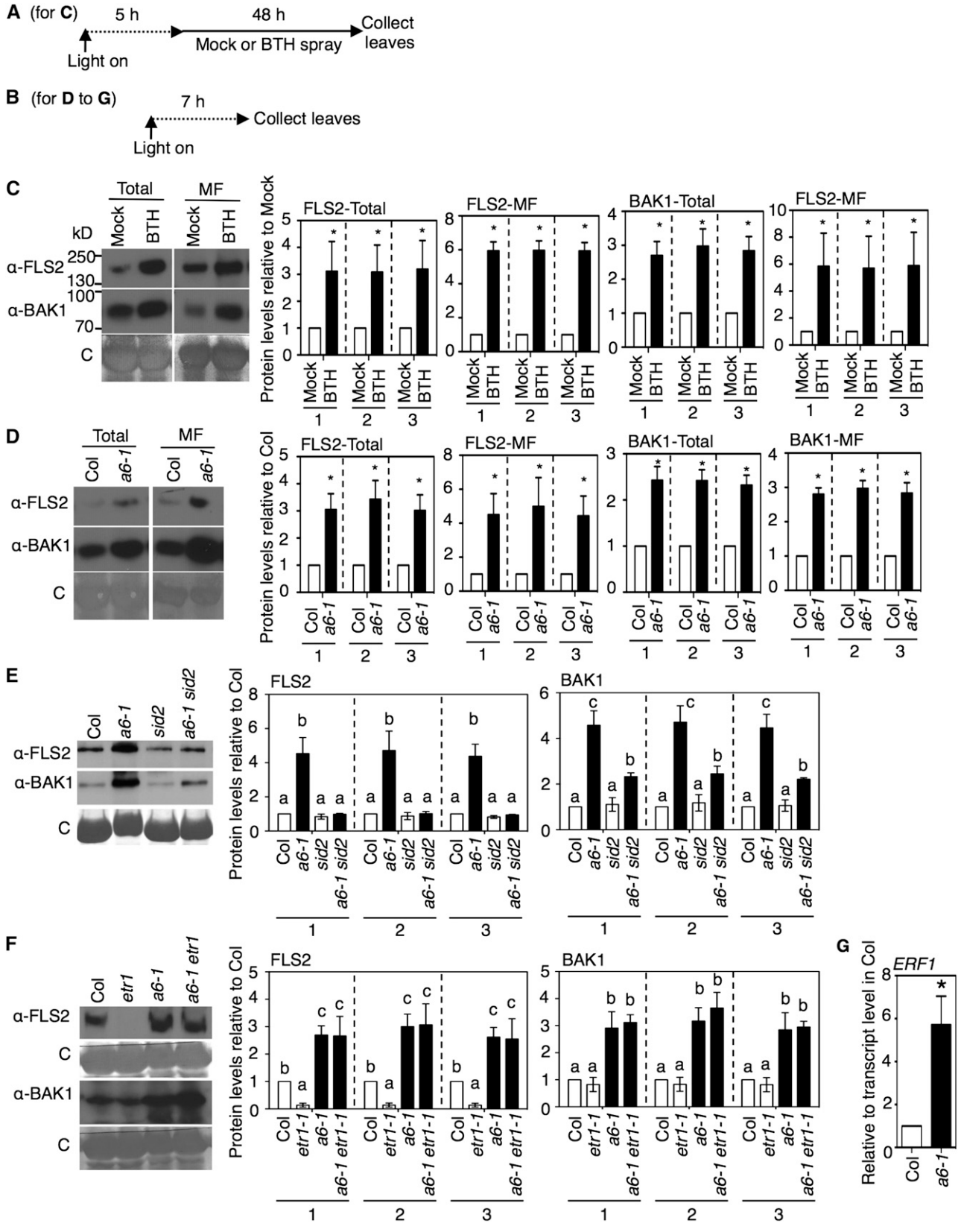

Figure 2. Effects of *acd6-1*, SA Accumulation, and/or SA Agonist Treatment on PAMP (Co)Receptor Levels.

incubated in water overnight prior to flg22 treatment, there was no evidence for FLS2-BAK1 complexes in mock-treated *acd6-1*. Furthermore, 10 min after the flg22 treatment, the FLS2 signal was weaker in *acd6-1* than in Col (Supplemental Figure 3). Thus, long water treatment (16 h) interrupts FLS2-BAK1 complex formation in *acd6-1*, similar to other phenotypes.

In conclusion, these experiments show that BAK1 and FLS2 contribute to a subset of autoimmune phenotypes in *acd6-1* plants that do not involve the activation of MPKs or the formation of high levels of FLS2-BAK1 complexes.

SA and BTH Confer PRR-Dependent Signaling Independent of an Added PAMP Stimulus

To test whether SA contributed to the same autoimmunity phenotypes as FLS2 and BAK1, we compared the status of defense signaling markers in *acd6-1* and *acd6-1 sid2-1* plants. Indeed, *acd6-1 sid2-1* plants showed suppression of defenses often associated with BAK1 and FLS2 activity (Figures 3D to 3F). By contrast, *acd6-1 etr1-1* double mutants that have the same level of SA (and FLS2; Figure 2F) as *acd6-1* (Lu et al., 2009) showed the same level of basal callose deposition as *acd6-1* (Figure 3E).

We next tested the possibility that treatment of wild-type plants with an SA agonist is sufficient to activate BAK1- and FLS2-dependent defenses known be induced by flg22 in *Arabidopsis*, including ROS accumulation, MAPK activation, and callose deposition (Figures 4A to 4C).

Consistent with previous reports using BTH and/or SA (Beckers et al., 2009; Sato et al., 2010; Xu et al., 2014), BTH treatment did not stimulate MAPK activity or ROS accumulation in our growth conditions within 10 or 30 min, respectively (Supplemental Figures 4A and 4B). Even after 24 h, there was no MAPK activation (Beckers et al., 2009) or ROS accumulation (Figure 1J).

BTH did induce callose deposition (Figure 4D), in agreement with a previous study (Kohler et al., 2002). Interestingly, this induction was partially dependent on the presence of functional FLS2, BAK1, and ACD6 proteins, as the respective loss-of-function (or reduced-function) single mutants (*fls2-1*, *bak1-4*, and *acd6-2*) showed less callose deposition than the wild type in response to BTH (Figure 4D). Additionally, BTH-induced callose deposition was reduced in the *etr1-1* mutant that has lower FLS2 levels or in the SA signaling mutant *npr1-1* but not in the *sid2-1* or *mpk3* mutant (Figure 4D). Basal levels of ACD6 are lower in *npr1-1* plants than in the wild type (Lu et al., 2003), which may explain the reduced callose response of *npr1-1* in response to BTH. These data show that the induction of callose deposition by BTH involves FLS2, BAK1, NPR1, and ACD6 but not MPK3 or SID2.

Previously, it was shown that flg22 treatment causes reduced FLS2 levels and a period of nonresponsiveness to secondary flg22 treatment (Flury et al., 2013; Smith et al., 2014). As BTH triggered FLS2- and BAK1-dependent signaling to induce callose, we checked whether, like flg22, BTH caused short-term downregulation of the receptors. Indeed, within 4 h, BTH caused reduced FLS2 and BAK1 levels (Figure 4E). The FLS2 level was also reduced 4 h after BTH treatment by the spraying method (Supplemental Figure 1K), which was also used for the 24- and 48-h BTH treatments in Figure 2C and Supplemental Figure 1I. As a result, plants treated with BTH were less responsive to secondary flg22 treatments, as evidenced by dampened ROS accumulation and callose deposition (Figures 4F and 4G). We ruled out the possibility that BTH interferes with the detection of ROS by showing that we could detect H_2O_2 in the presence of BTH (Supplemental Figure 5A). Additionally, a solution of flg22 and BTH induced the same level of ROS accumulation as a solution of flg22 (Supplemental Figure 5B). This indicates that BTH did not directly interfere with flg22 action. Together, these data show that BTH causes some events that are similar to those induced by flg22, including callose deposition, transiently reduced FLS2 and BAK1 levels, and attenuated responsiveness to flg22.

SA Regulates the PAMP Receptor CERK1

To determine whether SA might regulate additional PRRs, we studied the effect of BTH and *acd6-1* on levels of CERK1, the chitin and peptidoglycan receptor and coreceptor, respectively, of *Arabidopsis* (Petutschnig et al., 2010; Willmann et al., 2011). Figures 5A to 5E show the experimental designs for these measurements.

CERK1 levels were increased in the microsomal fraction prepared from *acd6-1* (Figure 5F) and wild-type leaves treated

Figure 2. (continued).

(A) and **(B)** Chemical treatment and plant tissue collection schemes for the indicated panels: **(A)** for **(C)**; **(B)** for **(D)** to **(F)**.

(C) FLS2 and BAK1 protein levels after BTH treatment of the wild type (Col). Leaves were collected 48 h after spray treatment with 100 μM BTH or mock treatment. Total and microsomal fraction (MF) proteins isolated from plants were analyzed by immunoblotting with FLS2 and BAK1 antibodies.

(D) FLS2 and BAK1 protein levels in Col and *acd6-1* (*a6-1*). Proteins were extracted and analyzed as in **(C)**.

(E) and **(F)** Effects of *sid2-1* and *etr1-1* mutations on FLS2 and BAK1 protein levels in *acd6-1*. Microsomal proteins isolated from Col, *acd6-1*, *sid2-1*, *acd6-1 sid2-1*, *etr1-1*, and *acd6-1 etr1-1* plants were analyzed as in **(C)**.

(G) Transcript level of *ERF1*, an ethylene-responsive marker gene, in *acd6-1* relative to the wild type determined by qRT-PCR using three biological repeats.

Graphs in **(C)** to **(F)** show the mean fold change in receptor levels (normalized to total protein [1], Rubisco [2], or all proteins except Rubisco [3]) of the indicated plants relative to mock **(C)** or the wild type (Col) (**[D]** to **[F]**), quantified from immunoblots using three independent experiments. Dotted lines in **(C)** and **(D)** indicate separate comparisons with the respective mock **(C)** and Col **(D)** values in the total and microsomal fraction, respectively. Error bars show SE. *$P < 0.05$; letters above bars represent significance groups as determined by the Newman-Keuls multiple comparison test, $P < 0.05$ or better (**[E]** and **[F]**). C, Coomassie blue stained. These experiments were repeated three times with similar results.

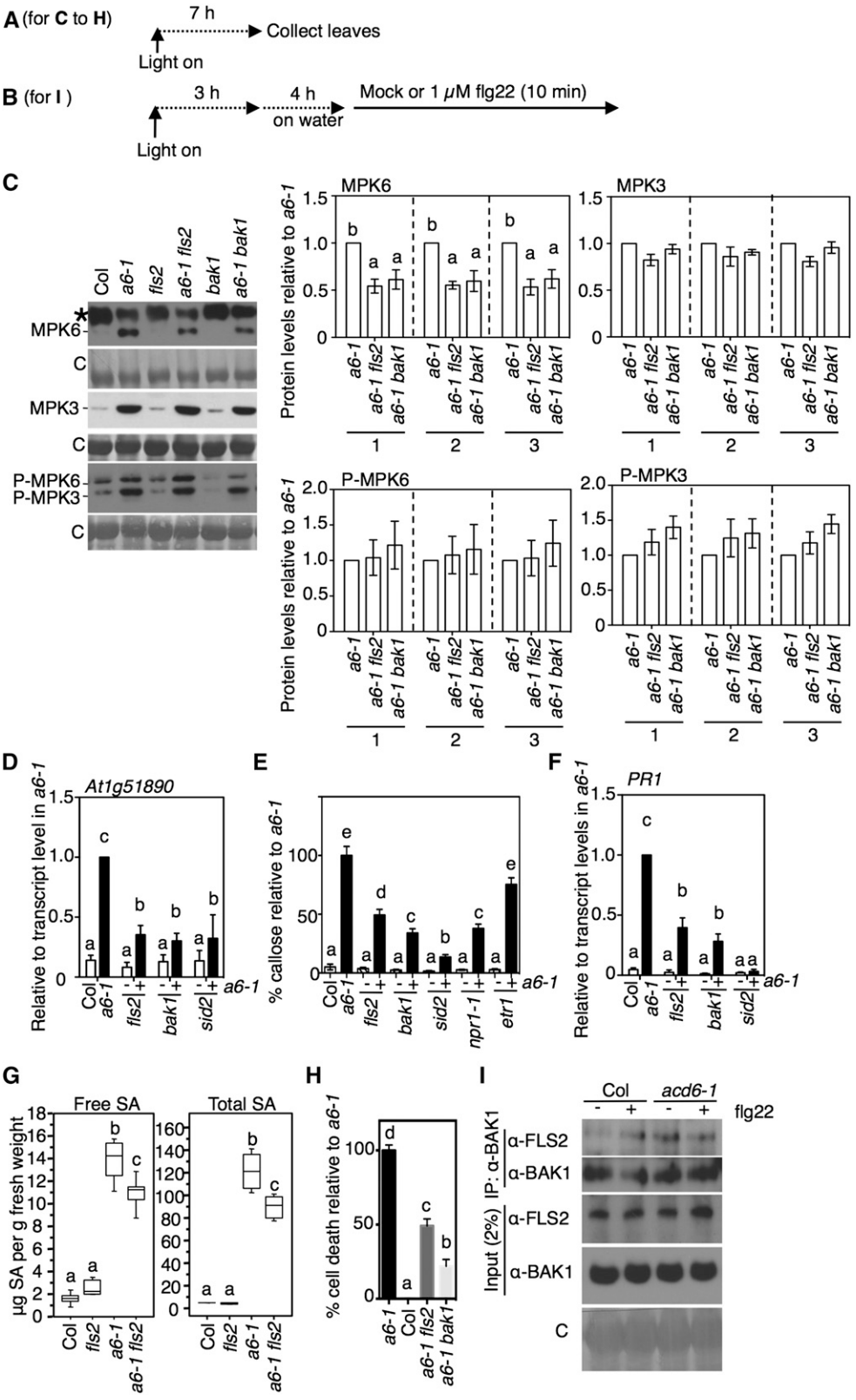

Figure 3. Analysis of Defenses in *acd6-1* Single and Double Mutants.

for 48 h with BTH (Figure 5G) relative to microsomes from untreated wild-type and mock-treated wild-type plants, respectively. *acd6-1 sid2-1* plants accumulated less CERK1 than *acd6-1* (Figure 5F), but the CERK1 level in *acd6-1 sid2-1* was still modestly elevated relative to *sid2-1* (Figure 5F, graphs). Additionally, chitin-induced callose deposits in *acd6-1* (Figure 5H) and wild-type plants pretreated for 24 h with BTH (Figure 1I) were also enhanced relative to wild-type and mock-treated wild-type plants, respectively. Thus, SA regulates CERK1 protein accumulation in a manner similar to FLS2 and BAK1 and causes an enhancement of responsiveness to chitin. *cerk1* plants accumulated less callose than wild-type plants upon BTH treatment, similar to the phenotype of *fls2*, *bak1-4*, and *acd6-2* mutants (Figure 4D). A 4-h treatment with BTH, but not flg22, caused a 50% reduction in the CERK1 levels (Figure 5I) and reduced responsiveness to chitin treatment for callose accumulation (Figure 5J). Thus, several PAMP receptors are regulated by SA and also contribute to BTH-induced callose in the absence of PRR ligands.

ACD6 Contributes to PAMP Responses and Regulates Basal FLS2, BAK1, and CERK1 Levels

Since the gain-of-function *acd6-1* mutant showed enhanced PAMP responses and ACD6 associates with FLS2 (Zhang et al., 2014), it seemed possible that ACD6 might have a role in PRR-related responses. To test this, we first monitored the ability of PAMP response-inducing bacteria to colonize ACD6-deficient plants (*acd6-2*). For this purpose, we used *hrcC*$^{-}$ *P. syringae*, a strain that induces PAMP responses but cannot secrete effectors that suppress PAMP responses (Alfano and Collmer, 1997). Spray-inoculated *acd6-2* plants were more highly colonized with *hrcC*$^{-}$ *P. syringae* than wild-type plants after 3 d, similar to the phenotype of *fls2* plants (Figure 6A). *acd6-2* plants also showed a reduction in the responses to flg22 treatment similar to those seen in *bak1-4*, including accumulation of ROS production, the *At1g51890* transcript, and callose deposition (Figures 6B to 6D). The PAMP response defects in *acd6-2* were also similar to those seen in *sid2-1* plants, except that in *sid2-1* ROS accumulation was not affected (Figures 6B to 6D). Chitin-induced callose was also reduced in *acd6-2* (Figure 6E). Basal microsomal membrane levels of FLS2, BAK1, and CERK1 were lower in *acd6-2* than in the wild type (Figure 6F), which can explain the reduced responsiveness of *acd6-2* to PAMPs.

As ACD6 is required for callose deposition with BTH (Figure 4D), it seemed possible that ACD6 might have a role in regulating flg22 responses after BTH treatment. Indeed, in *acd6-2*, flg22-induced ROS accumulation and callose deposits were not reduced 4 h after samples were treated with BTH (Figures 6G to 6J). These data show that ACD6 is needed for restricting the growth of *hrcC*$^{-}$ *P. syringae*, regulating responsiveness to flg22 and/or chitin under different conditions and regulating the membrane levels of three PRRs.

ACD6 Associates with BAK1 and CERK1

ACD6 associates with FLS2 (Zhang et al., 2014). The effect of ACD6 on PRR responses might be through the formation of ACD6-FLS2 and additional complexes. To test whether additional complexes can form, we used a coimmunoprecipitation approach and plants that express functional hemagglutinin (HA)-tagged ACD6 (Lu et al., 2005). We confirmed that the ACD6-HA plants showed dynamic changes in CERK1 abundance after spray treatment with BTH (Supplemental Figure 6). When ACD6-HA was immunoprecipitated, we found that both BAK1 and CERK1 were copurified (Figure 7). Thus, the effects of ACD6 on signaling are likely through a direct effect on multiple PRR complexes.

Figure 3. (continued).

(A) and **(B)** Chemical treatment and plant collection schemes for the indicated panels: **(A)** for **(C)** to **(H)**; **(B)** for **(I)**.

(C) MPK levels and MPK activity analysis in the indicated plants, immunodetected in total protein extracts by MPK3, MPK6, and phospho-p44/42 MPK antibodies. The assignment of the phosphorylated MPK3 band was confirmed using *acd6-1 mpk3* plants (Supplemental Figure 2). The star indicates a background band. C, Coomassie blue stained.

(D) Transcript levels of the flg22-inducible gene *At1g51890* in the indicated plants relative to *acd6-1* (*a6-1*) determined by qRT-PCR.

(E) Callose deposition in leaves of the indicated plant lines ($n > 8$) from a representative experiment.

(F) Transcript levels of *PR1* (an output of SA signaling) in the indicated plants relative to *acd6-1* determined by qRT-PCR.

In **(D)** to **(F)**, – or + indicates the absence or presence of *acd6-1*. These experiments were repeated three times with similar results.

(G) Total and free SA levels were quantified from the indicated plant lines. Box plots show the median, the second and third quartiles, which indicate 50% of the data points (open boxes), and the range (vertical lines above and below the boxes; $n = 6$). Letters above each box represent significance groups as determined by Fisher's protected least significance measure, a posthoc multiple *t* test, $P < 0.001$.

(H) Cell death in *acd6-1*, *acd6-1 fls2*, and *acd6-1 bak1-4* mutants is shown as a percentage of the area of cell death in *acd6-1*. In different experiments, there was 18 to 26% area of cell death per viewing field in *acd6-1*. Each genotype was tested at least in two independent experiments. Letters above bars represent significance groups as determined by the Newman-Keuls multiple comparison test ($n \geq 15$). Each letter group differs from other letter groups at $P < 0.05$ or better.

In **(D)**, **(F)**, and **(H)**, error bars show SE using three or more independent experiments analyzed together. Graphs in **(C)** show the mean fold change in MPK/phospho-MPK levels (normalized to total protein [1], Rubisco only [2], or all proteins except Rubisco [3]) of the indicated plants relative to *acd6-1* quantified from immunoblots using three independent experiments. Letters above bars in **(C)** to **(F)** and **(H)** represent significance groups as determined by the Newman-Keuls test, $P < 0.05$ or better.

(I) FLS2-BAK1 complexes in the wild type (Col) and *acd6-1* with water pretreatment and mock (−) or 1 μM flg22 (+) treatment for 10 min. Top, BAK1-containing complexes immunoprecipitated with BAK1 antibody, separated by SDS-PAGE, and subjected to immunoblot analysis with FLS2 and BAK1 antibodies. Bottom, FLS2 and BAK1 protein levels from total proteins of the indicated plants. This experiment was repeated four times with similar results. Complex formation of FLS2-BAK1 in mock treatment was not seen when tissue was incubated overnight in water (Supplemental Figure 3).

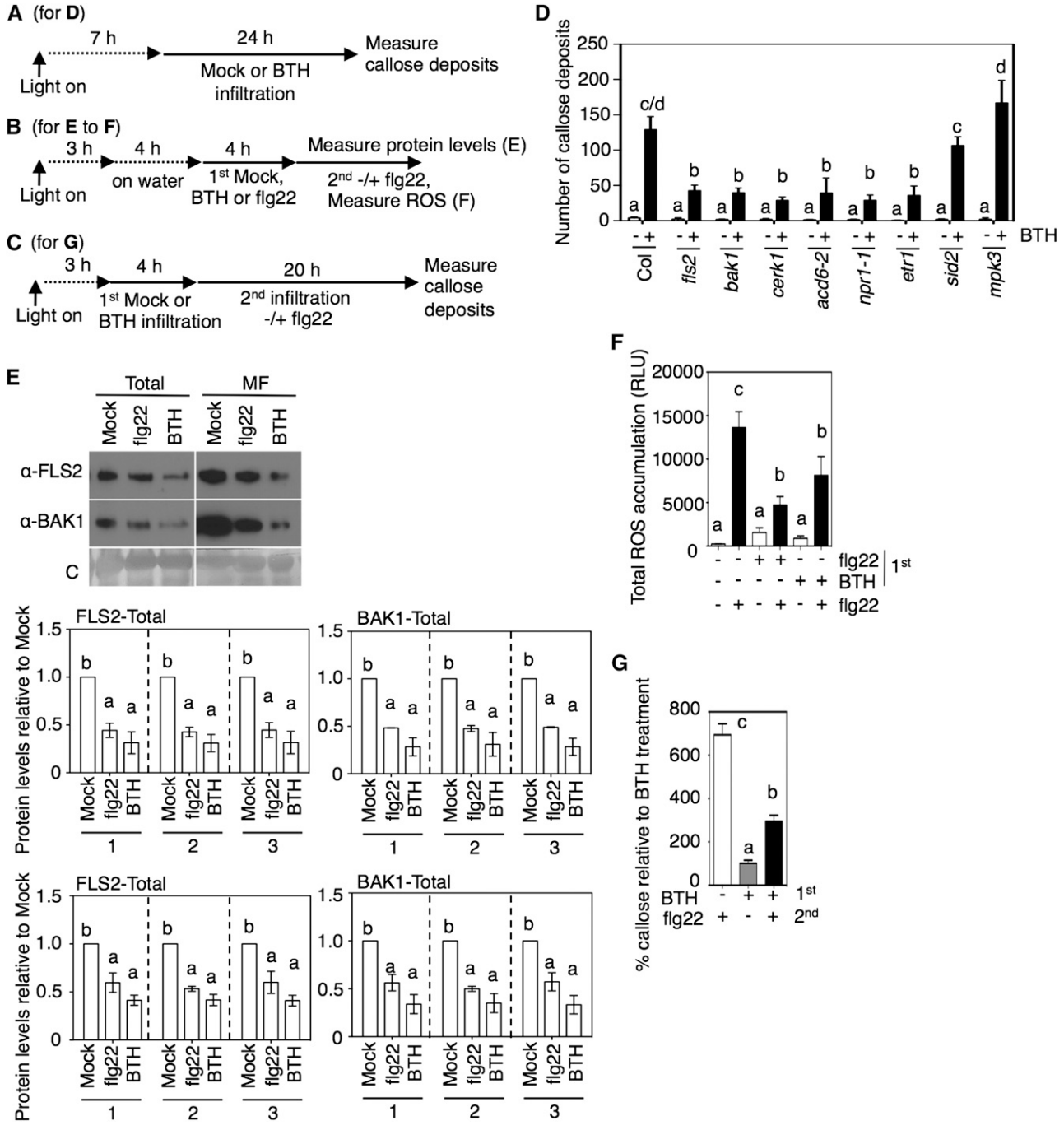

Figure 4. Short-Term Effects of the SA Agonist BTH on Receptor-Dependent Signaling.

(A) to **(C)** Chemical treatment and plant collection schemes for the indicated panels: **(A)** for **(D)**; **(B)** for **(E)** and **(F)**; **(C)** for **(G)**.

(D) Callose deposition 24 h after mock or 100 μM BTH treatment in leaves of the indicated plants ($n > 8$). – or + indicates the absence or presence of BTH.

(E) FLS2 and BAK1 protein levels in total or microsomal fraction (MF) from wild-type (Col) plant leaves 4 h after water, 1 μM flg22, or 100 μM BTH treatment. Graphs show the average fold change in receptor levels (normalized to total protein [1], Rubisco only [2], or all proteins except Rubisco [3]) of the indicated plants relative to mock treatment quantified from immunoblots using three independent experiments. Error bars indicate SE. C, Coomassie blue stained.

(F) ROS accumulation after flg22 treatment of leaves pretreated for 4 h with BTH or flg22 ($n > 10$). RLU, relative light units.

(G) Callose deposition in leaves infiltrated with water (−), 1 μM flg22 (flg22 +), or 100 μM BTH (BTH +). Callose was detected 20 h after the second treatment and is shown as a percentage of callose in plants ($n > 8$) treated only with BTH.

In **(D)** to **(G)**, letters above bars represent significance groups as determined by the Newman-Keuls multiple comparison test, $P < 0.05$ or better. Error bars in **(D)**, **(F)**, and **(G)** are SD from data from representative experiments. These experiments were repeated three times with similar results.

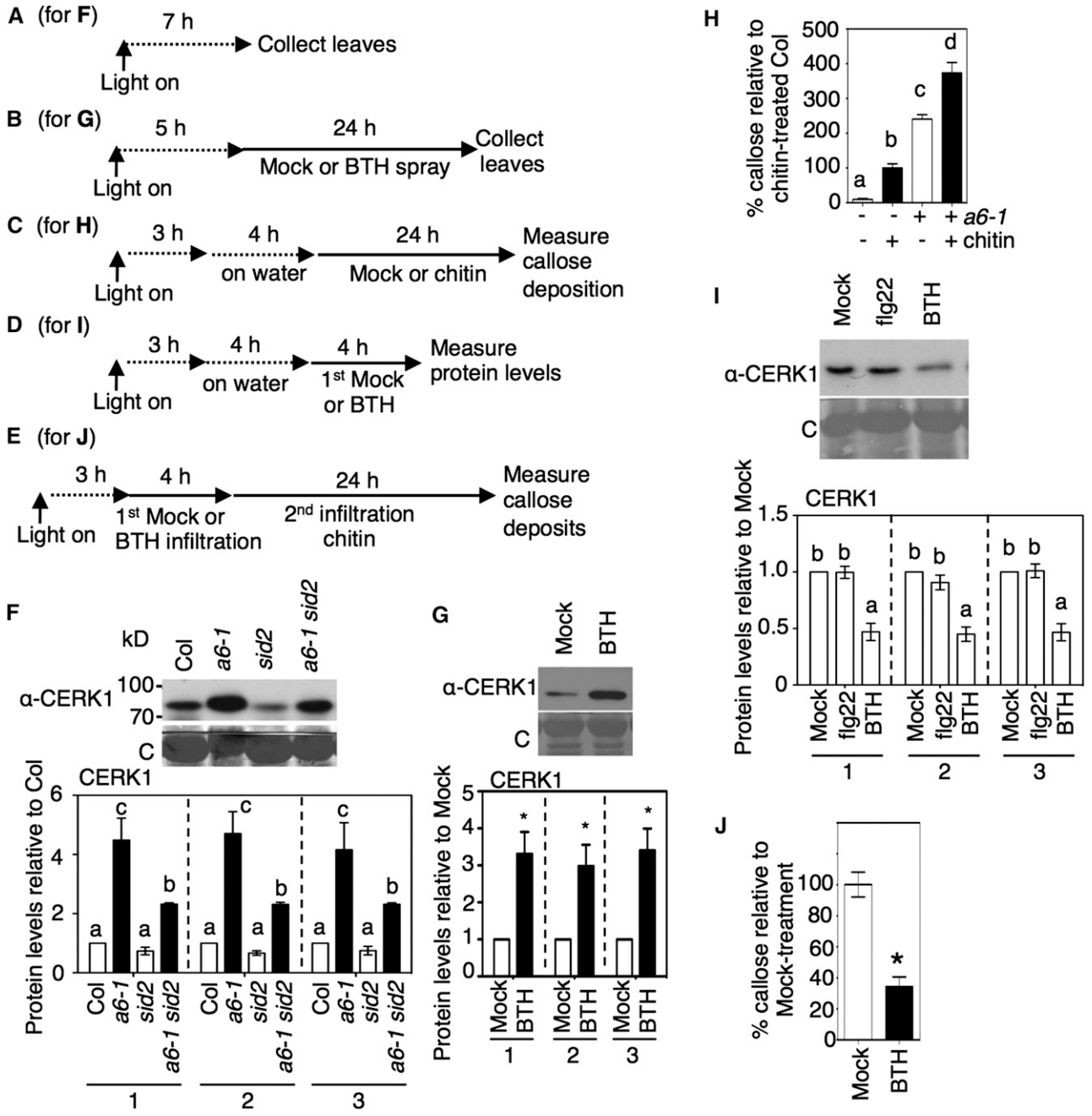

Figure 5. Effects of SA Accumulation or the SA Agonist BTH on CERK1, Another PAMP Receptor.

(A) to **(E)** Chemical treatment and plant collection schemes for the indicated panels: **(A)** for **(F)**; **(B)** for **(G)**; **(C)** for **(H)**; **(D)** for **(I)**; **(E)** for **(J)**.

(F) Effects of *acd6-1* and SID2 on CERK1 protein levels. Microsomal proteins isolated from wild-type (Col), *acd6-1* (*a6-1*), *sid2-1*, and *acd6-1 sid2-1* plants were analyzed by immunoblotting with CERK1 antibody.

(G) CERK1 protein level after BTH treatment of the wild type (Col). Leaves were collected 48 h after treatment with 100 μM BTH or mock treatment. Proteins were extracted from microsomal fraction and analyzed as in **(F)**.

(H) Callose deposition in leaves of the indicated plant lines ($n > 24$) as a percentage of wild-type (Col) plants treated with 10 μg/mL chitin. – or + indicates without or with *acd6-1* and absence or presence of chitin.

(I) CERK1 protein levels in microsomal fraction from wild-type (Col) leaves 4 h after water, 1 μM flg22, or 100 μM BTH treatment as in Figure 4E.

(J) Callose deposition in leaves infiltrated with 10 μg/mL chitin after pretreatment with water (−) or 100 μM BTH (BTH +). Callose was detected 24 h after the second treatment and is shown as a percentage of callose in plants ($n > 24$) given mock treatment.

Graphs in **(F)**, **(G)**, and **(I)** show the mean levels of CERK1 (normalized to total protein [1], Rubisco only [2], or all proteins except Rubisco [3]) of the indicated plants relative to Col **(F)** or mock (**[G]** and **[I]**) quantified from immunoblots using three independent experiments. C, Coomassie blue stained. In **(F)** to **(J)**, error bars show SE. *$P < 0.05$; letters above bars represent significance groups as determined by the Newman-Keuls multiple comparison test, $P < 0.05$ or better.

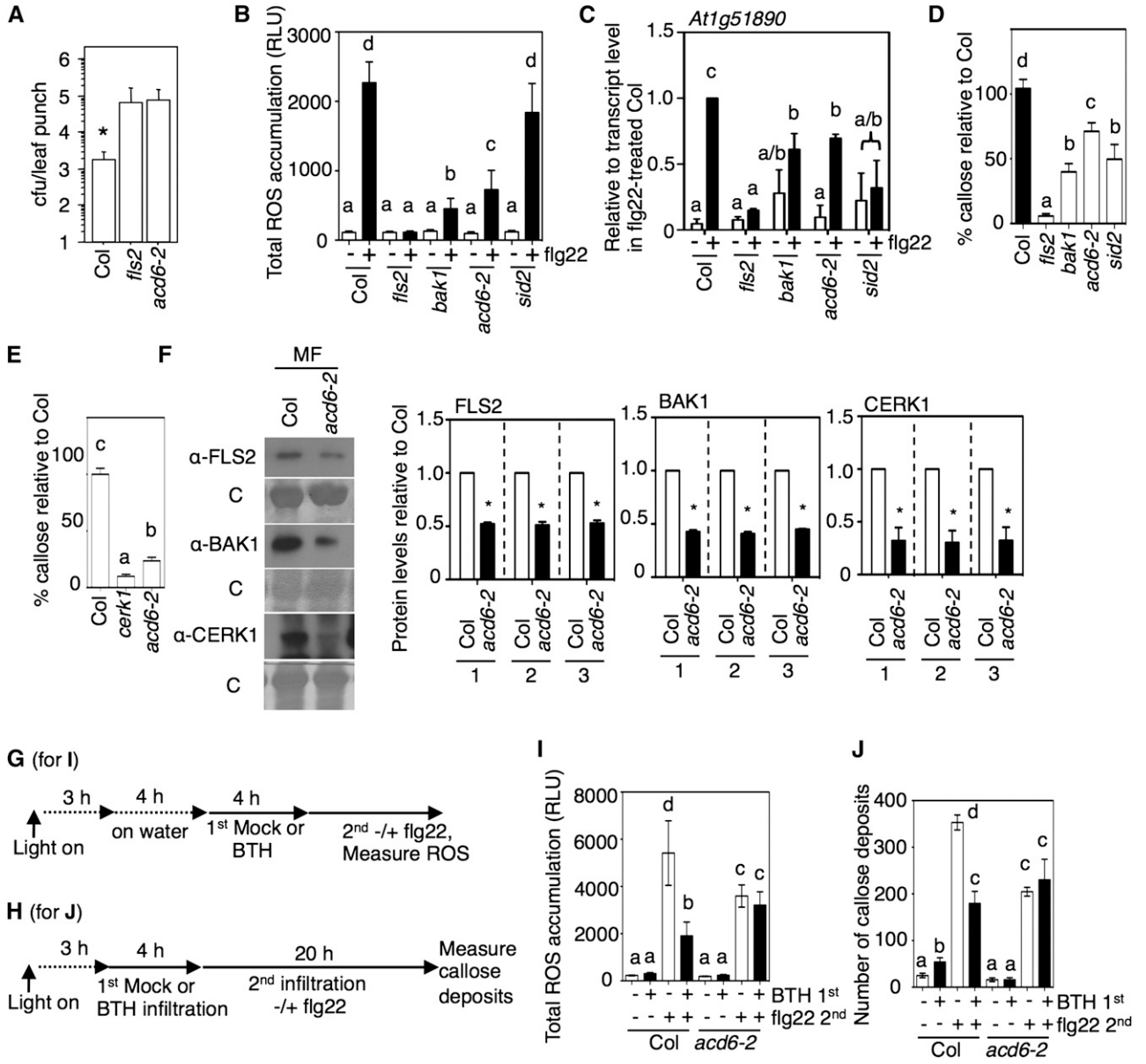

Figure 6. The *acd6* Null Mutant Shows Decreased Responses to flg22 and Reduced Receptor Levels.

(A) Increased colonization of type III secretion-deficient *P. syringae* in plants lacking ACD6. The *acd6-2* mutant and the wild type (Col) were sprayed with *P. syringae* pv *maculicola* ES4326 *hrcC*$^{-}$ at a dose of OD_{600} = 0.03, and 3 d later, bacteria were enumerated from eight leaf discs per genotype. *fls2* was included as a control for increased colonization. Colonization of mutant plants was higher than that seen in the wild type (*P < 0.04, *t* test). cfu, colony-forming units.

(B) to **(D)** Analysis of *acd6-2* in comparison with *fls2*, *bak1-4*, and *sid2-1*. – or + indicates the absence or presence of flg22 in **(B)** and **(C)**.

(B) Total ROS accumulation after 1 μM flg22 treatment (as in Figures 1A and 1E) in the indicated plants ($n > 10$). RLU, relative light units.

(C) Transcript levels of the flg22-induced gene *At1g51890* in the indicated plants relative to wild-type (Col) plants 1 h after infiltration with 1 μM flg22 determined by qRT-PCR.

(D) and **(E)** Callose deposition 18 h after 1 μM flg22 ($n = 8$) **(D)** or 24 h after 10 μg/mL chitin ($n > 24$) **(E)** infiltration in leaves of the indicated plant lines as a percentage of callose in the wild type (Col).

(F) FLS2, BAK1, and CERK1 protein levels are low in the membrane microsomal fraction (MF) of *acd6-2* relative to wild-type plants. Microsomal fraction proteins isolated from plants were analyzed by immunoblotting with FLS2, BAK1, and CERK1 antibodies. Graphs show the mean fold change in receptor levels (normalized to total protein [1], Rubisco only [2], or all proteins except Rubisco [3]) of *acd6-2* relative to the wild type (Col) quantified using immunoblots using three independent experiments. *P < 0.05, which indicates that the *acd6-2* values were different from wild-type values.

(G) and **(H)** Chemical treatment schemes for the indicated panels: **(G)** for **(I)**; **(H)** for **(J)**. In **(G)**, "on water" indicates that tissue was excised and floated on water to facilitate BTH uptake.

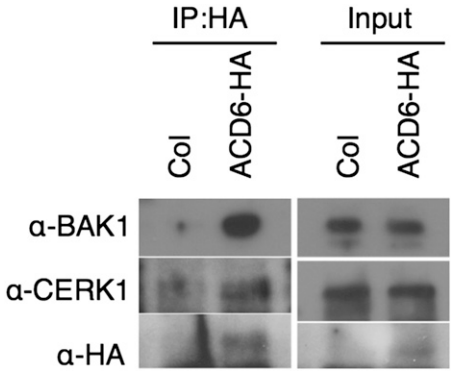

Figure 7. BAK1 and CERK1 Form Complexes with ACD6 in ACD6-HA Plants.

Left, ACD6-containing complexes immunoprecipitated with HA matrix, separated by SDS-PAGE, and subjected to immunoblot analysis with BAK1 and CERK1 antibodies. Right, protein levels from microsomal proteins. The wild type (Col) was used as a negative control. This experiment was repeated three times with similar results.

DISCUSSION

This work revealed several aspects of FLS2, BAK1, and CERK1 regulation and PAMP-independent signaling roles for these PRRs. Receptor levels are regulated by ACD6, possibly through direct PRR-ACD6 associations (Zhang et al., 2014; this work). They are also dynamically regulated by SA signaling: early after SA agonist treatments (4 h), FLS2, BAK1, and CERK1 are downregulated, whereas later (24 to 48 h), their levels in the membrane increase. These changes in levels are paralleled by altered responsiveness of plants to PAMPs. ACD6 is needed to attenuate the responsiveness to flg22 after 4 h of BTH treatment. Two types of experiments indicate PAMP-independent signaling roles for FLS2, BAK1, and/or CERK1. First, these PRRs and ACD6 are needed for maximal callose induction in response to the SA agonist BTH. Second, FLS2 and BAK1 contribute to several constitutive defense phenotypes of the gain-of-function *acd6-1* mutant. Thus, FLS2, BAK1, ACD6, and SA are part of a regulatory cycle that affects receptor levels and signaling. CERK1 is also subject to at least part of this regulatory cycle.

Ethylene is an important factor in the regulation of basal levels of FLS2 protein and transcript levels (Boutrot et al., 2010; Mersmann et al., 2010). Our experiments show that ethylene signaling is not always obligatory for FLS2 expression, as FLS2 levels remain high in *acd6-1 etr1* plants in which ethylene perception is blocked. In the case of *acd6-1*, elevated SA production confers increased receptor levels and probably accounts for the fact that ethylene perception is dispensable. Other scenarios in which SA signaling is high may also alleviate the need for ethylene signaling to regulate FLS2 and possibly other receptors. Interestingly, FLS2 and BAK1 show ACD6-dependent increased plasma membrane pools in response to 48 h of SA agonist treatment (Zhang et al., 2014). Thus, SA signaling can maximize a defense system by increasing the accumulation of PAMP-related (co)receptors.

SA signaling confers enhanced defense responses when future infections or infection-related stimuli occur (Lawton et al., 1996; Katz et al., 1998; Tsuda et al., 2008; Beckers et al., 2009). Given the observation that within 1 d after BTH treatment the levels of PRRs are increased, previous studies showing SA-mediated potentiation of flg22 responses (Sato et al., 2010; Xu et al., 2014) can probably be explained by higher levels of PAMP receptors. This agrees well with the observation that overexpression of FLS2 confers increased responsiveness to flg22 (Gómez-Gómez and Boller, 2000).

A short time after treatment (within 4 h), BTH transiently downregulates several PRRs, similar to desensitization caused by ligand-activated receptors that undergo endocytosis (Robatzek et al., 2006). It is not known if reduction of PRR levels in response to BTH also results from endocytosis or from the induction of proteasome activity or the unfolded protein response, both of which can be activated by SA (Moreno et al., 2012; Pu and Bassham, 2013; Üstün et al., 2013).

PAMP receptor signaling starts with the extracellular perception of ligands (Chinchilla et al., 2006). Our experiments do not address whether PRR-dependent signaling in response to SA or BTH occurs through an event(s) that is extracellular or intracellular. It is unclear if the effects of SA or BTH on receptors on the cell surface are similar to ligand perception. Since FLS2, BAK1, and CERK1 are involved, a common feature of all three proteins may be important. One possibility is that their intracellular kinase domains may be affected in a similar way. Interestingly, SA can activate the adenosine monophosphate-activated protein kinase in human embryonic kidney 293 cells (Hawley et al., 2012). Additionally, Wang et al. (2013) reported that SA increases the intensity of callose staining and the concomitant partial restriction of plasmodesmata openings. In another study, FLS2-green fluorescent protein was seen to partially colocalize with sites of basal callose deposition that appear to be in positions of plasmodesmata (punctate structures along the plasma membrane; Faulkner et al., 2013). It seems possible that PRRs (FLS2, BAK1, and CERK1) together with ACD6 form a signaling platform(s) that is needed for the callose response to SA/BTH. Whether this may occur at plasmodesmata sites and/or some other subcellular site (s) remains to be determined.

Signaling outputs that result from flg22 treatment, including MAPK activation and the production of ROS, result from a branched pathway (Smith et al., 2014). For example, flg22-induced ROS production (Mersmann et al., 2010) does not require MPK3

Figure 6. (continued).

(I) ROS accumulation after flg22 treatment of Col or *acd6-2* leaves pretreated for 4 h with BTH or flg22 ($n > 10$).

(J) Callose deposition in leaves infiltrated with water (−), 1 μM flg22 (flg22 +), or 100 μM BTH (BTH +). Callose was detected 20 h after the second treatment in plants ($n > 8$).

Error bars in **(A)**, **(B)**, **(D)**, **(I)**, and **(J)** show SD from one representative experiment. Error bars in **(C)**, **(E)**, and **(F)** show SE of three independent experiments analyzed together. Letters above bars represent significance groups as determined by the Newman-Keuls multiple comparison test, $P < 0.05$. These experiments were repeated three times with similar results.

or MPK6, despite their activation. Therefore, it is possible that the signaling outputs in response to flg22 and BTH only partially overlap. As mentioned above, treatment of plants with flg22 or BTH has the shared effect that they both cause downregulation of one or more PRRs and induce callose deposition. However, responses to these stimuli show some differences: FLS2 is absolutely needed for all flg22 responses (Boutrot et al., 2010; Mersmann et al., 2010), whereas FLS2 is only quantitatively needed for BTH-induced callose. BAK1 is quantitatively required for responses to both stimuli, which may be related to the presence of other family members (Chinchilla et al., 2007; Heese et al., 2007; Schwessinger et al., 2011; Belkhadir et al., 2012) or other PRRs. Treatment with flg22, but not BTH, induces ROS and MAPK activation. Conversely, treatment with BTH causes downregulation of CERK1 levels, whereas treatment with flg22 does not. The limited shared signaling outputs that are activated in response to flg22 and BTH likely reflect different mechanisms by which PRRs participate in signaling after the respective treatments. Although several PRRs contribute to callose induction in response to BTH, there may be additional effects of BTH/SA signaling that confer disease resistance in a manner that is independent of PRRs.

Levels of pattern receptors affect the responsiveness of plants to PAMPs (Li et al., 2009; Boutrot et al., 2010), which in turn can affect susceptibility to different pathogens. The fact that ACD6 regulates the basal levels of FLS2, BAK1, and CERK1 may explain how natural variants of ACD6 confer increased resistance and/or autoimmune phenotypes (Todesco et al., 2010). Additionally, it seems likely that some proteins in the same family as ACD6 have similar functions in regulating the levels of receptors. Indeed, it is notable that loss of the predicted ACD6 family protein BDA1 results in hypersusceptibility to *hrcC*$^{-}$ *P. syringae* that can trigger PAMP signaling and suppresses the constitutive signaling of a gain-of-function mutation (*snc2-1D*) in a receptor-like membrane protein that lacks a kinase domain. Although BDA2 was suggested to function downstream of SNC2 (Yang et al., 2012), we suggest that BDA2 probably regulates the level of SNC2.

In summary, this work shows that the PRRs FLS2, BAK1, and CERK1 are involved in responses to both PAMPs and SA. Signaling upon flg22 perception involves the increased accumulation of SA (Mishina and Zeier, 2007; Tsuda et al., 2008). Other PAMPs induce the SA marker PR1 and, therefore, also are likely to cause increased SA levels (Gust et al., 2007; Tintor et al., 2013). We envision that PAMPs released from pathogens stimulate PRRs, resulting in higher levels of SA that is made in and/or mobilized to neighboring cells/tissues (Shulaev et al., 1995; Costet et al., 1999), stimulate ACD6 and PRR-dependent callose, and over time cause increased (co)receptor levels. This cycle provides a mechanism to ensure the amplification of local responses and enhanced responsiveness to future pathogen attacks.

METHODS

Plant Growth Conditions

All plants used in this study were derived from the *Arabidopsis thaliana* Col accession. Mutant and transgenic seeds used herein include previously described mutants and double mutants (*acd6-1*, *acd6-1 npr1-1*, *npr1-1*, *fls2*, *bak1-4*, *cerk1*, *acd6-2*, *sid2-1*, *acd6-1 sid2-1*, *etr1-1*, *acd6-1 etr1-1*, *mpk3*, and ACD6-HA) (Chang et al., 1993; Cao et al., 1994; Nawrath and Métraux, 1999; Rate et al., 1999; Lu et al., 2005, 2009; Heese et al., 2007; Miya et al., 2007; Wang et al., 2007; Shan et al., 2008; Todesco et al., 2010). Double mutants *acd6-1 fls2*, *acd6-1 bak1-4*, and *acd6-1 mpk3* were obtained by doing crosses and screening the F2 generation for plants homozygous for *acd6-1* by PCR using derived cleaved-amplified polymorphic sequence markers (Rate et al., 1999) and using the respective gene-specific primers (*fls2*, 5′-AGGGCTTCTTACAAACCTTCG-3′ and 5′-CGTTGATGTTTTTGAACACCC-3′; *bak1-4*, 5′-CCTCCTATCTCTCCTAGACCGCCATC-3′ and 5′-CTCTTAAACAGGAGGCAACACTTCCA-3′; *mpk3*, 5′-TGCGCTTATTGACAGAGGTAA-3′ and 5′-CCGTATGTTGGATTGAGTGCT-3′) and the left border primer of the T-DNA (5′-ATTTTGCCGATTTCGGAAC-3′) for the second mutation. Plants were grown as described (Greenberg et al., 1994; Butt et al., 1998) in 16-h-light/8-h-dark conditions for 19 to 21 d and then harvested for various assays.

Chemical Treatment and Isolation of Total and Membrane Fractions

For immunoblot analysis with BTH (from Robert Dietrich, Syngenta)-treated samples, 20- to 21-d-old plants were sprayed with mock or 100 μM BTH until all the leaves were wet. Leaves (1 g) were collected 4 (Supplemental Figure 1K), 24, or 48 h after treatment with 100 μM BTH or mock treatment. For immunoprecipitation with BAK1 antibody or immunoblot analysis with 4-h BTH-treated samples in Figure 3I, Supplemental Figure 3, or Figure 4E, 1-g leaf samples of 20- to 21-d-old plants were excised, cut into 8- × 1-mm strips, floated on water for 4 h (Figures 3I and 4E) or 16 h (Supplemental Figure 3), and subsequently incubated with 1 μM flg22, 100 μM BTH, or water for 10 min or 4 h. For the immunoprecipitation with HA matrix, 5-g leaf samples from Col and ACD6-HA 20- to 21-d-old plants were collected.

All steps involved in total and membrane fractionation were performed at 4°C. Total extracts were isolated with immunoprecipitation buffer (as described by Chinchilla et al. [2007]; 50 mM Tris-HCl, pH 8.0, 10% glycerol, 0.5% sodium deoxycholate, 1% Igepal CA-630 from Sigma-Aldrich, and complete protease inhibitor cocktail from Roche). To isolate membrane fractions, 1 g of leaf tissue was homogenized with grinding buffer A (50 mM Tris-HCl, pH 7.5, 0.33 M sucrose, 5 mM EDTA, 150 mM NaCl, and complete protease inhibitor cocktail). The crude extracts were subjected to centrifugation at 10,000*g* for 10 min to pellet the insoluble material. The supernatant was further centrifuged at 100,000*g* for 60 min to obtain membrane and soluble fractions. Microsomal membranes in the pellet after 100,000*g* centrifugation were solubilized with resuspension in immunoprecipitation buffer.

Immunoblot Analysis and Immunoprecipitation

Solubilized total and microsomal membrane proteins were separated by SDS-PAGE. Primary antibodies used for immunoblots were as follows: FLS2 antibodies (rabbit [Chinchilla et al., 2007; Heese et al., 2007], 1:500 or 1:2500, respectively), BAK1 antibodies (rabbit [Chinchilla et al., 2007]; Agrisera/AS121858, 1:1000 or 1:6000), CERK1 antibody (rabbit [Petutschnig et al., 2010], 1:2500), and HA antibody (Covance/16B12, 1:1000). Secondary horseradish peroxidase-conjugated anti-mouse and anti-rabbit antibodies (Thermo Scientific) were used at 1:1000. SuperSignal West Pico Stable Peroxidase (Thermo Scientific) and SuperSignal West Femto Stable Peroxidase (Thermo Scientific) were used to detect the signals.

To determine MPK and phospho-MPK levels, total protein extract was prepared in grinding buffer A. MPK3 (Sigma-Aldrich), MPK6 (Sigma-Aldrich), and phospho-p44/42 MAPK (Erk1/2) (Thr202/Tyr204) (Cell Signaling Technologies) antibodies were used for immunoblotting (rabbit [Bartels et al., 2009; Beckers et al., 2009], 1:1000).

For the immunoprecipitation with BAK1 antibody, total extracts were incubated with 5 μL of BAK1 (rabbit; Chinchilla et al., 2007) or 2 μL of BAK1 (Agrisera/AS121858) antibodies and 50 μL of protein G agarose

(Roche) for 2 h at 4°C with gentle shaking. For the immunoprecipitation with HA matrix (Roche), microsomal fractions from 5 g of leaves were incubated with 100 μL of HA matrix for 2 h at 4°C with gentle shaking. Immunoblot analyses were performed with FLS2, BAK1, CERK1, and HA antibodies.

Quantitation of Immunoblot Membranes

Bradford assays were used to quantify protein levels in extracts and ensure equal loading of total proteins for gels used for immunoblot analysis. FLS2, BAK1, CERK1, MPK3, MPK6, and phospho-MPK3/6 levels were subsequently quantified using Gel-Pro analyzer densitometry software from three independent immunoblots. Protein levels were normalized in three different ways using Coomassie Brilliant Blue R 250-stained membranes: relative to the total protein content (labeled as method 1 on graphs), the Rubisco content (labeled as method 2 on graphs), or all proteins except Rubisco (labeled as method 3 on graphs). All three methods gave similar results.

RNA Preparation and cDNA Synthesis

For Figures 2G, 3D, and 3F, 0.5 g of leaves was collected from wild-type and *acd6-1* plants. For Figure 6C, water or 1 μM flg22 was infiltrated into four leaves. Total RNA preparations were performed using Trizol reagent (Invitrogen). cDNA synthesis was performed using Prime Masterscript (Takara).

Real-Time RT-PCR Analyses

SYBR Green Master ROX reagent (Roche) and the Applied Biosystems 7900HT Fast Real-Time PCR system were used for quantitative RT-PCR (qRT-PCR). Real-time RT-PCR was performed as described (Tateda et al., 2011). Primer sets used for ERF1 (forward, 5′-GGAAACACTCGATGAGACGG-3′; reverse, 5′-CAACCACTTCAAACTTAAGGTCCC-3′) or previously described primers (*At1g51890*, *PR1*, and *CBP20*) (Lu et al., 2003; He et al., 2006; Tateda et al., 2011) were used. The amount of cDNA was calculated relative to the signals of a standard dilution of the respective PCR products using SDS2.3 software (Applied Biosystems). Transcript levels of defense-related genes normalized to the level of *CBP20* (Tateda et al., 2011) were determined by qRT-PCR using three biological replicates each composed of three plants per genotype or treatment.

Callose Quantitation

Callose deposits were stained with aniline blue as described (Kim and Mackey, 2008) except that chlorophyll was cleared using methanol: acetone (3:1). Leaves from at least eight independent plants for each genotype were used for measurements. Callose, quantified by manually counting deposits in photographs, is presented as a percentage of deposits found in *acd6-1* or treated wild-type plants. To induce callose for Figures 1G and 5H, leaves were floated on water, 300 nM flg22, or 10 μg/mL chitin (Sigma-Aldrich/C9752). For Figures 4D, 4G, 5J, 6D, and 6J, water, 100 μM BTH, 1 μM flg22, or 10 μg/mL chitin was infiltrated into leaves. For Figure 1I, water, 100 μM BTH, 1 μM flg22, or 10 μg/mL chitin was infiltrated 24 h after mock or BTH spraying of leaves.

SA Measurements

Free and total SA was measured by HPLC (Agilent Technologies 1200 Series) from 0.1 g of leaf tissue as described previously (Lu et al., 2003; Song et al., 2004) using anisic acid as an internal control.

ROS Accumulation Measurements

Prior to BTH or flg22 treatment, leaf discs from plants 19 to 21 d old first were floated on water for 4 h on 96-well plates; longer times were avoided to minimize the effects of water treatment. To detect ROS after 4-h treatments with flg22 or BTH, leaves were incubated with water, 1 μM flg22, or 100 μM BTH. ROS was measured after adding luminol solution (34 μg/mL luminol, 20 μg/mL peroxidase, and either water or 1 μM flg22) with a microplate reader (Tecan Safire2; Tecan) as described (Schwessinger et al., 2011). In Supplemental Figure 1E, leaf discs were floated on water for 4, 5, or 12 h and ROS was detected with flg22 as described above. To detect H_2O_2 or ROS induced by flg22 with BTH (Supplemental Figure 5), ROS was detected by luminol solution, which included luminol, peroxidase, water or 100 μM BTH, and water, 0.3% H_2O_2, or 1 μM flg22. Total ROS was measured for 30 min.

Pseudomonas syringae Infections

Plants were spray-inoculated with *P. syringae* pv *maculicola* ES4326 *hrcC*$^-$ at OD_{600} = 0.03 and sampled 3 or 4 d after inoculation to determine the level of colonization as described previously (Jelenska et al., 2010). Eight leaves were sampled for each plant genotype.

Accession Numbers

Sequence data from this article can be found in the GenBank/EMBL data libraries under accession numbers At5g46330 (*FLS2*), At4g33430 (*BAK1*), At4g14400 (*ACD6*), At3g21630 (*CERK1*), At1g74710 (*SID2*), At1g66340 (*ETR1*), At3g23240 (*ERF1*), At3g45640 (*MPK3*), At2g43790 (*MPK6*), At1g64280 (*NPR1*), and At2g14610 (*PR1*). Accession numbers for T-DNA lines are SALK_141277 (*fls2*), SALK_116202 (*bak1-4*), SALK_045869 (*acd6-2*), SALK_151594 (*mpk3*), CS3726 (*npr1-1*), and CS237 (*etr1-1*).

Supplemental Data

The following materials are available in the online version of this article.

Supplemental Figure 1. Effect of BTH, *acd6-1*, or Water Treatment on PAMP (Co)Receptor Levels.

Supplemental Figure 2. Verification That *acd6-1* Has Elevated MPK3 Levels.

Supplemental Figure 3. FLS2-BAK1 Complexes Induced by flg22 Are Less Stable in *acd6-1*.

Supplemental Figure 4. MPK Activity and ROS Accumulation Are Not Induced by BTH.

Supplemental Figure 5. BTH Has No Effect on ROS Measurements.

Supplemental Figure 6. Confirmation That Plants That Express ACD6-HA Show Normal Regulation of CERK1 after BTH Treatment.

ACKNOWLEDGMENTS

We thank the Ohio State Stock Center and A. Heese, J.P. Rathjen, and V. Lipka for providing reagents. D.C. thanks Thomas Boller for his professional support. This work was supported by the National Institutes of Health (Grant R01 GM54292 to J.T.G.), the National Science Foundation (Grant IOS 0822393 to J.T.G.), the Swiss National Foundation (Grant 31003A-120655 to D.C.), and the Japan Society for the Promotion of Science (postdoctoral fellowships for research abroad to C.T.).

AUTHOR CONTRIBUTIONS

Z.Z., C.T., J.S., and J.T.G. designed the research. Z.Z., C.T., J.S., J.J., D.C., and J.T.G. performed the research and analyzed the data. C.T. and J.T.G. wrote the article with input from D.C., Z.Z., and J.J.

Received September 9, 2014; revised September 19, 2014; accepted September 27, 2014; published October 14, 2014.

REFERENCES

Alfano, J.R., and Collmer, A. (1997). The type III (Hrp) secretion pathway of plant pathogenic bacteria: Trafficking harpins, Avr proteins, and death. J. Bacteriol. **179:** 5655–5662.

Bartels, S., Anderson, J.C., González Besteiro, M.A., Carreri, A., Hirt, H., Buchala, A., Métraux, J.P., Peck, S.C., and Ulm, R. (2009). MAP kinase phosphatase1 and protein tyrosine phosphatase1 are repressors of salicylic acid synthesis and SNC1-mediated responses in *Arabidopsis*. Plant Cell **21:** 2884–2897.

Beck, M., Zhou, J., Faulkner, C., MacLean, D., and Robatzek, S. (2012). Spatio-temporal cellular dynamics of the *Arabidopsis* flagellin receptor reveal activation status-dependent endosomal sorting. Plant Cell **24:** 4205–4219.

Beckers, G.J., Jaskiewicz, M., Liu, Y., Underwood, W.R., He, S.Y., Zhang, S., and Conrath, U. (2009). Mitogen-activated protein kinases 3 and 6 are required for full priming of stress responses in *Arabidopsis thaliana*. Plant Cell **21:** 944–953.

Belkhadir, Y., Jaillais, Y., Epple, P., Balsemão-Pires, E., Dangl, J.L., and Chory, J. (2012). Brassinosteroids modulate the efficiency of plant immune responses to microbe-associated molecular patterns. Proc. Natl. Acad. Sci. USA **109:** 297–302.

Berrocal-Lobo, M., Molina, A., and Solano, R. (2002). Constitutive expression of *ETHYLENE-RESPONSE-FACTOR1* in *Arabidopsis* confers resistance to several necrotrophic fungi. Plant J. **29:** 23–32.

Boller, T., and Felix, G. (2009). A renaissance of elicitors: Perception of microbe-associated molecular patterns and danger signals by pattern-recognition receptors. Annu. Rev. Plant Biol. **60:** 379–406.

Boudsocq, M., Willmann, M.R., McCormack, M., Lee, H., Shan, L., He, P., Bush, J., Cheng, S.H., and Sheen, J. (2010). Differential innate immune signalling via Ca^{2+} sensor protein kinases. Nature **464:** 418–422.

Boutrot, F., Segonzac, C., Chang, K.N., Qiao, H., Ecker, J.R., Zipfel, C., and Rathjen, J.P. (2010). Direct transcriptional control of the Arabidopsis immune receptor FLS2 by the ethylene-dependent transcription factors EIN3 and EIL1. Proc. Natl. Acad. Sci. USA **107:** 14502–14507.

Butt, A., Mousley, C., Morris, K., Beynon, J., Can, C., Holub, E., Greenberg, J.T., and Buchanan-Wollaston, V. (1998). Differential expression of a senescence-enhanced metallothionein gene in Arabidopsis in response to isolates of *Peronospora parasitica* and *Pseudomonas syringae*. Plant J. **16:** 209–221.

Cao, H., Bowling, S.A., Gordon, A.S., and Dong, X. (1994). Characterization of an *Arabidopsis* mutant that is nonresponsive to inducers of systemic acquired resistance. Plant Cell **6:** 1583–1592.

Chang, C., Kwok, S.F., Bleecker, A.B., and Meyerowitz, E.M. (1993). Arabidopsis ethylene-response gene ETR1: Similarity of product to two-component regulators. Science **262:** 539–544.

Chen, Y.Y., Lin, Y.M., Chao, T.C., Wang, J.F., Liu, A.C., Ho, F.I., and Cheng, C.P. (2009). Virus-induced gene silencing reveals the involvement of ethylene-, salicylic acid- and mitogen-activated protein kinase-related defense pathways in the resistance of tomato to bacterial wilt. Physiol. Plant. **136:** 324–335.

Chinchilla, D., Bauer, Z., Regenass, M., Boller, T., and Felix, G. (2006). The *Arabidopsis* receptor kinase FLS2 binds flg22 and determines the specificity of flagellin perception. Plant Cell **18:** 465–476.

Chinchilla, D., Zipfel, C., Robatzek, S., Kemmerling, B., Nürnberger, T., Jones, J.D., Felix, G., and Boller, T. (2007). A flagellin-induced complex of the receptor FLS2 and BAK1 initiates plant defence. Nature **448:** 497–500.

Conrath, U. (2011). Molecular aspects of defence priming. Trends Plant Sci. **16:** 524–531.

Conrath, U., Chen, Z., Ricigliano, J.R., and Klessig, D.F. (1995). Two inducers of plant defense responses, 2,6-dichloroisonicotinec acid and salicylic acid, inhibit catalase activity in tobacco. Proc. Natl. Acad. Sci. USA **92:** 7143–7147.

Costet, L., Cordelier, S., Dorey, S., Baillieul, F., Fritig, B., and Kauffmann, S. (1999). Relationship between localized acquired resistance (LAR) and the hypersensitive response (HR): HR is necessary for LAR to occur and salicylic acid is not sufficient to trigger LAR. Mol. Plant Microbe Interact. **12:** 655–662.

Delaney, T.P., Uknes, S., Vernooij, B., Friedrich, L., Weymann, K., Negrotto, D., Gaffney, T., Gut-Rella, M., Kessmann, H., Ward, E., and Ryals, J. (1994). A central role of salicylic acid in plant disease resistance. Science **266:** 1247–1250.

Faulkner, C., Petutschnig, E., Benitez-Alfonso, Y., Beck, M., Robatzek, S., Lipka, V., and Maule, A.J. (2013). LYM2-dependent chitin perception limits molecular flux via plasmodesmata. Proc. Natl. Acad. Sci. USA **110:** 9166–9170.

Felix, G., Duran, J.D., Volko, S., and Boller, T. (1999). Plants have a sensitive perception system for the most conserved domain of bacterial flagellin. Plant J. **18:** 265–276.

Flury, P., Klauser, D., Schulze, B., Boller, T., and Bartels, S. (2013). The anticipation of danger: Microbe-associated molecular pattern perception enhances AtPep-triggered oxidative burst. Plant Physiol. **161:** 2023–2035.

Friedrich, L., et al. (1996). A benzothiadiazole derivative induces systemic acquired resistance in tobacco. Plant J. **10:** 61–70.

Gómez-Gómez, L., and Boller, T. (2000). FLS2: An LRR receptor-like kinase involved in the perception of the bacterial elicitor flagellin in *Arabidopsis*. Mol. Cell **5:** 1003–1011.

Görlach, J., Volrath, S., Knauf-Beiter, G., Hengy, G., Beckhove, U., Kogel, K.H., Oostendorp, M., Staub, T., Ward, E., Kessmann, H., and Ryals, J. (1996). Benzothiadiazole, a novel class of inducers of systemic acquired resistance, activates gene expression and disease resistance in wheat. Plant Cell **8:** 629–643.

Greenberg, J.T., Guo, A., Klessig, D.F., and Ausubel, F.M. (1994). Programmed cell death in plants: A pathogen-triggered response activated coordinately with multiple defense functions. Cell **77:** 551–563.

Gust, A.A., Biswas, R., Lenz, H.D., Rauhut, T., Ranf, S., Kemmerling, B., Götz, F., Glawischnig, E., Lee, J., Felix, G., and Nürnberger, T. (2007). Bacteria-derived peptidoglycans constitute pathogen-associated molecular patterns triggering innate immunity in Arabidopsis. J. Biol. Chem. **282:** 32338–32348.

Hawley, S.A., et al. (2012). The ancient drug salicylate directly activates AMP-activated protein kinase. Science **336:** 918–922.

He, P., Shan, L., Lin, N.C., Martin, G.B., Kemmerling, B., Nürnberger, T., and Sheen, J. (2006). Specific bacterial suppressors of MAMP signaling upstream of MAPKKK in *Arabidopsis* innate immunity. Cell **125:** 563–575.

Heese, A., Hann, D.R., Gimenez-Ibanez, S., Jones, A.M., He, K., Li, J., Schroeder, J.I., Peck, S.C., and Rathjen, J.P. (2007). The receptor-like kinase SERK3/BAK1 is a central regulator of innate immunity in plants. Proc. Natl. Acad. Sci. USA **104:** 12217–12222.

Hsu, F.C., Chou, M.Y., Chou, S.J., Li, Y.R., Peng, H.P., and Shih, M.C. (2013). Submergence confers immunity mediated by the WRKY22 transcription factor in *Arabidopsis*. Plant Cell **25:** 2699–2713.

Jambunathan, N., Siani, J.M., and McNellis, T.W. (2001). A humidity-sensitive *Arabidopsis* copine mutant exhibits precocious cell death and increased disease resistance. Plant Cell **13:** 2225–2240.

Jelenska, J., van Hal, J.A., and Greenberg, J.T. (2010). *Pseudomonas syringae* hijacks plant stress chaperone machinery for virulence. Proc. Natl. Acad. Sci. USA **107:** 13177–13182.

Jones, J.D., and Dangl, J.L. (2006). The plant immune system. Nature **444:** 323–329.

Katz, V.A., Thulke, O.U., and Conrath, U. (1998). A benzothiadiazole primes parsley cells for augmented elicitation of defense responses. Plant Physiol. **117:** 1333–1339.

Kim, M.G., and Mackey, D. (2008). Measuring cell-wall-based defenses and their effect on bacterial growth in *Arabidopsis*. Methods Mol. Biol. **415:** 443–452.

Kohler, A., Schwindling, S., and Conrath, U. (2002). Benzothiadiazole-induced priming for potentiated responses to pathogen infection, wounding, and infiltration of water into leaves requires the NPR1/NIM1 gene in Arabidopsis. Plant Physiol. **128:** 1046–1056.

Lawton, K.A., Friedrich, L., Hunt, M., Weymann, K., Delaney, T., Kessmann, H., Staub, T., and Ryals, J. (1996). Benzothiadiazole induces disease resistance in Arabidopsis by activation of the systemic acquired resistance signal transduction pathway. Plant J. **10:** 71–82.

Li, J., Zhao-Hui, C., Batoux, M., Nekrasov, V., Roux, M., Chinchilla, D., Zipfel, C., and Jones, J.D. (2009). Specific ER quality control components required for biogenesis of the plant innate immune receptor EFR. Proc. Natl. Acad. Sci. USA **106:** 15973–15978.

Love, A.J., Laval, V., Geri, C., Laird, J., Tomos, A.D., Hooks, M.A., and Milner, J.J. (2007). Components of Arabidopsis defense- and ethylene-signaling pathways regulate susceptibility to *Cauliflower mosaic virus* by restricting long-distance movement. Mol. Plant Microbe Interact. **20:** 659–670.

Lu, H., Liu, Y., and Greenberg, J.T. (2005). Structure-function analysis of the plasma membrane-localized Arabidopsis defense component ACD6. Plant J. **44:** 798–809.

Lu, H., Rate, D.N., Song, J.T., and Greenberg, J.T. (2003). ACD6, a novel ankyrin protein, is a regulator and an effector of salicylic acid signaling in the *Arabidopsis* defense response. Plant Cell **15:** 2408–2420.

Lu, H., Salimian, S., Gamelin, E., Wang, G., Fedorowski, J., LaCourse, W., and Greenberg, J.T. (2009). Genetic analysis of *acd6-1* reveals complex defense networks and leads to identification of novel defense genes in Arabidopsis. Plant J. **58:** 401–412.

Mersmann, S., Bourdais, G., Rietz, S., and Robatzek, S. (2010). Ethylene signaling regulates accumulation of the FLS2 receptor and is required for the oxidative burst contributing to plant immunity. Plant Physiol. **154:** 391–400.

Mishina, T.E., and Zeier, J. (2007). Pathogen-associated molecular pattern recognition rather than development of tissue necrosis contributes to bacterial induction of systemic acquired resistance in *Arabidopsis*. Plant J. **50:** 500–513.

Miya, A., Albert, P., Shinya, T., Desaki, Y., Ichimura, K., Shirasu, K., Narusaka, Y., Kawakami, N., Kaku, H., and Shibuya, N. (2007). CERK1, a LysM receptor kinase, is essential for chitin elicitor signaling in *Arabidopsis*. Proc. Natl. Acad. Sci. USA **104:** 19613–19618.

Moore, J.W., Loake, G.J., and Spoel, S.H. (2011). Transcription dynamics in plant immunity. Plant Cell **23:** 2809–2820.

Moreno, A.A., Mukhtar, M.S., Blanco, F., Boatwright, J.L., Moreno, I., Jordan, M.R., Chen, Y., Brandizzi, F., Dong, X., Orellana, A., and Pajerowska-Mukhtar, K.M. (2012). IRE1/bZIP60-mediated unfolded protein response plays distinct roles in plant immunity and abiotic stress responses. PLoS ONE **7:** e31944.

Mosher, S., Moeder, W., Nishimura, N., Jikumaru, Y., Joo, S.H., Urquhart, W., Klessig, D.F., Kim, S.K., Nambara, E., and Yoshioka, K. (2010). The lesion-mimic mutant *cpr22* shows alterations in abscisic acid signaling and abscisic acid insensitivity in a salicylic acid-dependent manner. Plant Physiol. **152:** 1901–1913.

Murphy, A.M., and Carr, J.P. (2002). Salicylic acid has cell-specific effects on tobacco mosaic virus replication and cell-to-cell movement. Plant Physiol. **128:** 552–563.

Nawrath, C., and Métraux, J.P. (1999). Salicylic acid induction-deficient mutants of *Arabidopsis* express PR-2 and PR-5 and accumulate high levels of camalexin after pathogen inoculation. Plant Cell **11:** 1393–1404.

Petutschnig, E.K., Jones, A.M., Serazetdinova, L., Lipka, U., and Lipka, V. (2010). The lysin motif receptor-like kinase (LysM-RLK) CERK1 is a major chitin-binding protein in *Arabidopsis thaliana* and subject to chitin-induced phosphorylation. J. Biol. Chem. **285:** 28902–28911.

Pu, Y., and Bassham, D.C. (2013). Links between ER stress and autophagy in plants. Plant Signal. Behav. **8:** e24297.

Ranf, S., Eschen-Lippold, L., Pecher, P., Lee, J., and Scheel, D. (2011). Interplay between calcium signalling and early signalling elements during defence responses to microbe- or damage-associated molecular patterns. Plant J. **68:** 100–113.

Rate, D.N., Cuenca, J.V., Bowman, G.R., Guttman, D.S., and Greenberg, J.T. (1999). The gain-of-function *Arabidopsis acd6* mutant reveals novel regulation and function of the salicylic acid signaling pathway in controlling cell death, defenses, and cell growth. Plant Cell **11:** 1695–1708.

Robatzek, S., Chinchilla, D., and Boller, T. (2006). Ligand-induced endocytosis of the pattern recognition receptor FLS2 in Arabidopsis. Genes Dev. **20:** 537–542.

Sato, M., Tsuda, K., Wang, L., Coller, J., Watanabe, Y., Glazebrook, J., and Katagiri, F. (2010). Network modeling reveals prevalent negative regulatory relationships between signaling sectors in Arabidopsis immune signaling. PLoS Pathog. **6:** e1001011.

Schulze, B., Mentzel, T., Jehle, A.K., Mueller, K., Beeler, S., Boller, T., Felix, G., and Chinchilla, D. (2010). Rapid heteromerization and phosphorylation of ligand-activated plant transmembrane receptors and their associated kinase BAK1. J. Biol. Chem. **285:** 9444–9451.

Schwessinger, B., Roux, M., Kadota, Y., Ntoukakis, V., Sklenar, J., Jones, A., and Zipfel, C. (2011). Phosphorylation-dependent differential regulation of plant growth, cell death, and innate immunity by the regulatory receptor-like kinase BAK1. PLoS Genet. **7:** e1002046.

Shan, L., He, P., Li, J., Heese, A., Peck, S.C., Nürnberger, T., Martin, G.B., and Sheen, J. (2008). Bacterial effectors target the common signaling partner BAK1 to disrupt multiple MAMP receptor-signaling complexes and impede plant immunity. Cell Host Microbe **4:** 17–27.

Shulaev, V., Leon, J., and Raskin, I. (1995). Is salicylic acid a translocated signal of systemic acquired resistance in tobacco? Plant Cell **7:** 1691–1701.

Smith, J.M., Salamango, D.J., Leslie, M.E., Collins, C.A., and Heese, A. (2014). Sensitivity to Flg22 is modulated by ligand-induced degradation and de novo synthesis of the endogenous flagellin-receptor FLAGELLIN-SENSING2. Plant Physiol. **164:** 440–454.

Song, J.T., Lu, H., McDowell, J.M., and Greenberg, J.T. (2004). A key role for ALD1 in activation of local and systemic defenses in Arabidopsis. Plant J. **40:** 200–212.

Sun, Y., Li, L., Macho, A.P., Han, Z., Hu, Z., Zipfel, C., Zhou, J.M., and Chai, J. (2013). Structural basis for flg22-induced activation of the Arabidopsis FLS2-BAK1 immune complex. Science **342:** 624–628.

Tateda, C., Watanabe, K., Kusano, T., and Takahashi, Y. (2011). Molecular and genetic characterization of the gene family encoding the voltage-dependent anion channel in *Arabidopsis*. J. Exp. Bot. **62:** 4773–4785.

Tintor, N., Ross, A., Kanehara, K., Yamada, K., Fan, L., Kemmerling, B., Nürnberger, T., Tsuda, K., and Saijo, Y. (2013). Layered pattern receptor signaling via ethylene and endogenous elicitor peptides during Arabidopsis immunity to bacterial infection. Proc. Natl. Acad. Sci. USA **110:** 6211–6216.

Todesco, M., et al. (2010). Natural allelic variation underlying a major fitness trade-off in *Arabidopsis thaliana*. Nature **465:** 632–636.

Tsuda, K., Sato, M., Glazebrook, J., Cohen, J.D., and Katagiri, F. (2008). Interplay between MAMP-triggered and SA-mediated defense responses. Plant J. **53:** 763–775.

Üstün, S., Bartetzko, V., and Börnke, F. (2013). The *Xanthomonas campestris* type III effector XopJ targets the host cell proteasome to suppress salicylic-acid mediated plant defence. PLoS Pathog. **9:** e1003427.

Vanacker, H., Lu, H., Rate, D.N., and Greenberg, J.T. (2001). A role for salicylic acid and NPR1 in regulating cell growth in Arabidopsis. Plant J. **28:** 209–216.

Wang, H., Ngwenyama, N., Liu, Y., Walker, J.C., and Zhang, S. (2007). Stomatal development and patterning are regulated by environmentally responsive mitogen-activated protein kinases in *Arabidopsis*. Plant Cell **19:** 63–73.

Wang, Y., Bouwmeester, K., van de Mortel, J.E., Shan, W., and Govers, F. (2013). A novel Arabidopsis-oomycete pathosystem: Differential interactions with *Phytophthora capsici* reveal a role for camalexin, indole glucosinolates and salicylic acid in defence. Plant Cell Environ. **36:** 1192–1203.

Wildermuth, M.C., Dewdney, J., Wu, G., and Ausubel, F.M. (2001). Isochorismate synthase is required to synthesize salicylic acid for plant defence. Nature **414:** 562–565.

Willmann, R., et al. (2011). Arabidopsis lysin-motif proteins LYM1 LYM3 CERK1 mediate bacterial peptidoglycan sensing and immunity to bacterial infection. Proc. Natl. Acad. Sci. USA **108:** 19824–19829.

Xu, J., Xie, J., Yan, C., Zou, X., Ren, D., and Zhang, S. (2014). A chemical genetic approach demonstrates that MPK3/MPK6 activation and NADPH oxidase-mediated oxidative burst are two independent signaling events in plant immunity. Plant J. **77:** 222–234.

Yang, Y., Zhang, Y., Ding, P., Johnson, K., Li, X., and Zhang, Y. (2012). The ankyrin-repeat transmembrane protein BDA1 functions downstream of the receptor-like protein SNC2 to regulate plant immunity. Plant Physiol. **159:** 1857–1865.

Yoshioka, K., Kachroo, P., Tsui, F., Sharma, S.B., Shah, J., and Klessig, D.F. (2001). Environmentally sensitive, SA-dependent defense responses in the cpr22 mutant of Arabidopsis. Plant J. **26:** 447–459.

Zhang, Z., Shrestha, J., Tateda, C., and Greenberg, J.T. (2014). Salicylic acid signaling controls the maturation and localization of the Arabidopsis defense protein ACCELERATED CELL DEATH6. Mol. Plant **7:** 1365–1383.

Zhou, F., Menke, F.L., Yoshioka, K., Moder, W., Shirano, Y., and Klessig, D.F. (2004). High humidity suppresses ssi4-mediated cell death and disease resistance upstream of MAP kinase activation, H_2O_2 production and defense gene expression. Plant J. **39:** 920–932.

Zipfel, C., Kunze, G., Chinchilla, D., Caniard, A., Jones, J.D., Boller, T., and Felix, G. (2006). Perception of the bacterial PAMP EF-Tu by the receptor EFR restricts Agrobacterium-mediated transformation. Cell **125:** 749–760.